BULLETIN OF THE EARTHQUAKE
RESEARCH INSTITUTE
Vol. 47 (1969), pp. 31-41

2. World-wide Distribution of the Group Velocity of Rayleigh Wave as Determined by Dispersion Data.

By Yasuo SATÔ,
Earthquake Research Institute,
and
Tetsuo SANTÔ,
International Institute of Seismology and Earthquake Engineering.
(Read Nov. 26, 1968.—Received Nov. 30, 1968.)

Abstract

The group velocity of Rayleigh wave all over the world is expressed by spherical surface harmonics with the coefficients determined by the least square method, the data being the microfilm seismogram of WWSSN. Using the same coefficients the Rayleigh wave velocity is again synthesized and its distribution is compared with the topography, which was also synthesized by means of spherical surface harmonics.

1. Introduction

The study of surface wave dispersion has been carried out by many seismologists and a large number of papers were published concerning the distribution of Rayleigh- and Love-wave velocity.[1] The present work is one of the investigations in this direction based on a somewhat different method of calculations; namely the distribution of the (reciprocal of) group velocity of Rayleigh waves is expressed by means of spherical surface harmonics all over the world and their coefficients are determined by the method of least squares. Thus a most probable velocity distribu-

1) M. T. PORKA, "Surface Wave Studies on the Crust and Upper Mantle in Eurasia," *Institute of Seismology, Univ. of Helsinki*, Publ. No. 90.

T. SANTÔ, "Lateral Variation of Rayleigh Wave Dispersion Character. Part II." *Pure and Appl. Geophys.*, **62** (1965), 67.

R. L. KOVACH, "Seismic Surface Waves: Some Observations and Recent Development," *Physics and Chemistry of the Earth*, Vol. 6 (Pergamon Press), p. 1.

T. SANTÔ and Y. SATÔ, "World-wide Survey of the Regional Characteristics of Group Velocity Dispersion of Rayleigh Waves," *Bull. Earthq. Res. Inst.*, **44** (1966), 939.

T. SANTÔ, "Lateral Variation of Rayleigh Wave Dispersion Character. Part V. North American Continent and Arctic Ocean," *Bull. Earthq. Res. Inst.*, **46** (1968), 431.

tion is obtained using all the available observations, without assuming the boundary of regional velocity classification in advance.

2. Analysis

The travel time between the epicenter Q and the observation point P is given by an expression

$$t=\int_{(QP)} \frac{d\Delta}{v(\theta,\varphi)}, \tag{1}$$

where the velocity v is a function of the location on the surface. (θ : colatitude, φ : longitude). The integration path is, forgetting the refraction effect in the horizontal surface, the geodetic line connecting Q and P.* If $1/v(\theta,\varphi)$ is expanded into a series of spherical surface harmonics

$$\begin{aligned}\frac{1}{v(\theta,\varphi)}=&\sum_{n=0}\sum_{m=0}^{h} A_n^m\cdot P_n^m(\cos\theta)\cdot\cos m\varphi\\&+\sum_{n=1}\sum_{m=0}^{n} B_n^m\cdot P_n^m(\cos\theta)\cdot\sin m\varphi.\end{aligned} \tag{2}$$

Corresponding to one earthquake we observe one travel time t_k at a station $P_k(k=1, 2, \cdots, N)$, hence introducing (2) into (1) the following equation is deduced.

$$\begin{aligned}t_k=&\sum_{n,m} A_n^m\cdot\int_{(QP_k)} P_n^m(\cos\theta)\cdot\cos m\varphi\, d\Delta\\&+\sum_{n,m} B_n^m\cdot\int_{(QP_k)} P_n^m(\cos\theta)\cdot\sin m\varphi\, d\Delta\end{aligned} \tag{3}$$

In this expression two integrals are functions of the epicenter location $Q(\Theta,\Phi)$ and the station location $P_k(\theta_k,\varphi_k)$, namely

$$\begin{aligned}t_k&=\sum_{n,m} A_n^m\cdot C_n^m(\Theta,\Phi;\theta_k,\varphi_k)\\&=\sum_{n,m} B_n^m\cdot S_n^m(\Theta,\Phi;\theta_k,\varphi_k)\end{aligned} \tag{4}$$

C_n^m and S_n^m can be numerically calculated if Θ, Φ and θ_k, φ_k are given. Consequently (4) is a linear algebraic equation with unknowns A_n^m and $B_n^m(n=0, 1, 2, \cdots; m=0, \cdots, n)$. Since there are many equations of this type $(k=1, 2, \cdots, N)$ we can determine the above unknowns using the

* The wave path F determined by Fermat's principle is not the geodetic line G. However, the travel time along F takes a stationary value, hence the travel time along G will differ only little from the observed value as long as G lies in the neighborhood of F.

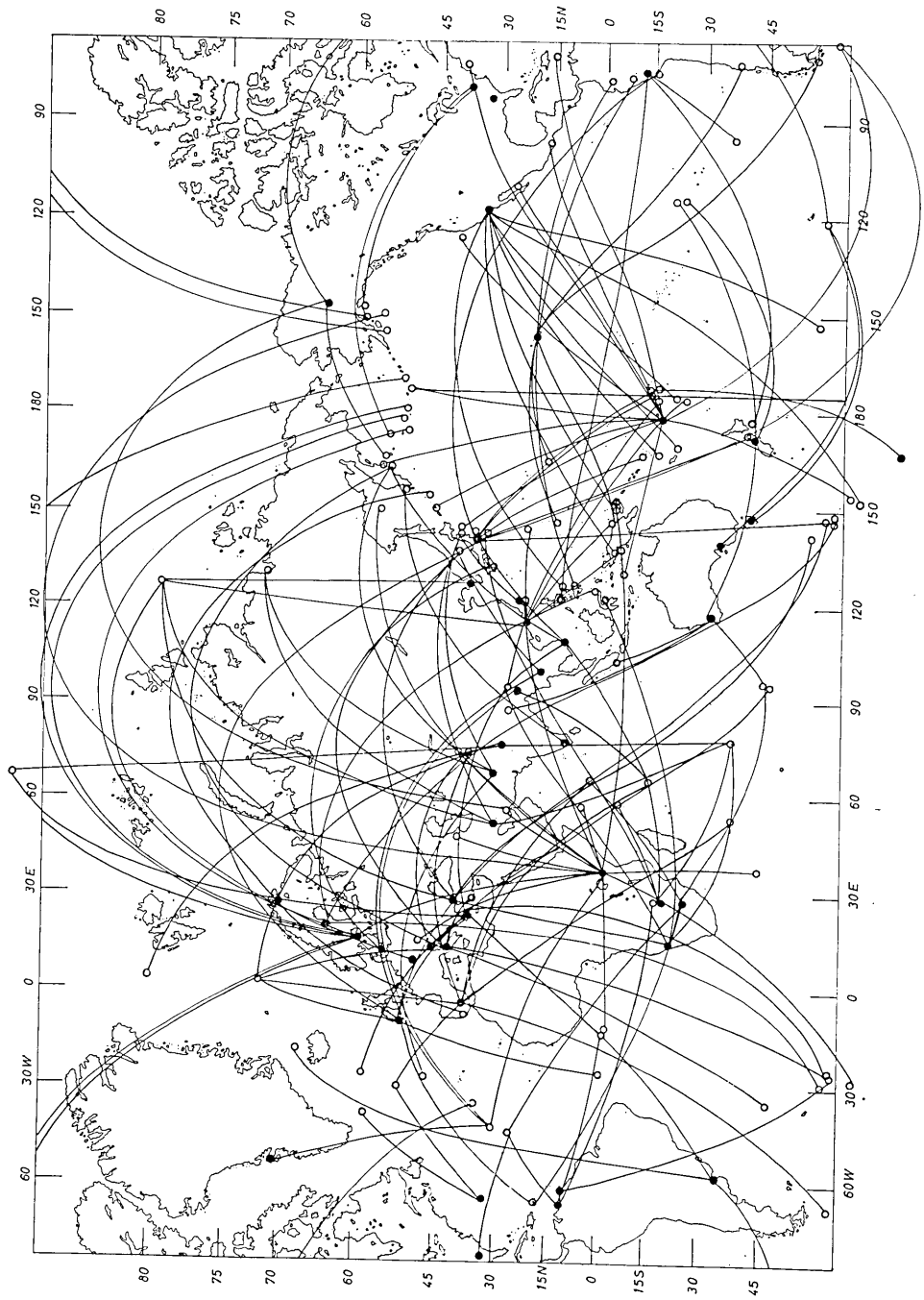

Fig. 1. Stations, epicenters and the connecting geodetic lines.

Table 1. Station, Epicenter and the travel time (period=30 sec.)

	STATION			EPICENTER		
	ABBRE-VIATION	LATI-TUDE	LONGI-TUDE	LATI-TUDE	LONGI-TUDE	TRAVEL TIME (SEC)
	ADE	-34.97	138.71	-56.00	-121.50	1892.
	ANP	25.18	121.52	39.50	141.80	737.
	AQU	42.35	13.42	-58.60	-25.50	3132.
	AQU	42.35	13.42	-46.70	-35.50	2943.
	AQU	42.35	13.42	35.50	28.70	454.
	AQU	42.35	13.42	40.40	138.90	2818.
	AQU	42.35	13.42	54.80	161.70	2681.
	ATL	33.43	-84.34	26.70	-44.60	1018.
	ATU	37.97	23.71	-58.50	-25.10	3118.
10	ATU	37.97	23.71	-1.90	-12.90	1636.
	ATU	37.97	23.71	28.10	93.80	2156.
	ATU	37.97	23.71	-15.00	66.80	2001.
	ATU	37.97	23.71	86.70	68.70	1649.
	BEC	32.38	-64.68	57.50	-38.50	885.
	BEC	32.38	-64.68	51.90	-30.00	922.
	BLA	37.21	-80.42	59.70	-147.00	1523.
	BLA	37.21	-80.42	53.60	172.10	2262.
	BUL	-20.14	28.61	33.40	141.80	3710.
	BUL	-20.14	28.61	-37.40	78.30	1366.
20	BUL	-20.14	28.61	5.70	58.00	1139.
	BUL	-20.14	28.61	-15.00	66.80	1111.
	CAR	10.51	-66.93	-16.60	28.80	2923.
	CAR	10.51	-66.93	-1.90	-12.90	1626.
	CAR	10.51	-66.93	26.70	-44.60	775.
	CHG	18.79	98.98	42.60	142.80	1477.
	CHG	18.79	98.98	30.60	-42.00	4232.
	CHR	-43.53	172.62	-25.00	-114.00	1875.
	COL	64.90	-147.81	35.20	-35.90	2082.
	COL	64.90	-147.81	27.50	55.90	2828.
30	COL	64.90	-147.81	55.20	165.20	836.
	COP	55.68	12.43	32.20	131.60	2477.
	GDH	69.25	-53.53	30.60	-42.00	1135.
	HKC	22.30	114.17	-3.50	135.50	1020.
	HKC	22.30	114.17	-3.00	145.50	1183.
	HKC	22.30	114.17	78.20	126.60	1875.
	HKC	22.30	114.17	28.10	93.80	687.
	HKC	22.30	114.17	22.00	144.00	815.
	HKC	22.30	114.17	-16.10	-176.90	2200.
	HKC	22.30	114.17	-24.00	-176.50	2430.
40	HNL	21.36	-157.81	19.00	146.00	1470.
	HNL	21.36	-157.81	-5.50	151.00	1617.
	HNL	21.36	-157.81	-1.00	-78.00	2250.
	HNL	21.36	-157.81	-7.80	-77.80	2320.
	HNL	21.36	-157.81	-54.00	-71.00	3000.
	HNL	21.30	-158.09	7.00	126.50	2085.
	HNL	21.36	-157.81	11.40	165.20	1016.
	HUA	-12.04	-75.32	13.50	121.00	4630.
	HUA	-12.04	-75.32	-41.00	175.80	2710.
	IST	41.04	28.98	-54.00	141.10	3926.
50	IST	41.04	28.98	40.40	138.90	2583.
	KEV	69.76	27.01	36.20	-7.60	1211.
	KEV	69.76	27.01	46.90	153.90	1866.
	KOD	10.23	77.47	51.80	156.80	2554.
	LPA	-34.91	-57.93	-56.00	-121.50	1408.
	LPA	-34.91	-57.93	67.20	-18.40	3153.
	LPA	-34.91	-57.93	-1.90	-12.90	1450.
	MAL	36.73	-4.41	2.90	65.70	2079.
	MAL	36.73	-4.41	72.20	1.70	1137.
	MAL	36.73	-4.41	51.90	-30.00	702.
60	MAL	36.73	-4.41	-37.20	52.20	2796.
	MAL	36.73	-4.41	-58.50	-66.20	3146.
	MAL	36.73	-4.41	-15.00	66.80	2554.
	MAL	36.73	-4.41	37.50	73.40	2043.
	MUN	-31.97	116.21	-22.30	-114.10	2985.
	MUN	-31.97	116.21	-45.20	96.40	561.
	MUN	-31.97	116.21	-5.50	102.50	840.
	MUN	-31.97	116.21	27.60	88.00	1978.
	NAI	-1.27	36.80	39.60	74.20	1762.
	NAI	-1.27	36.80	56.20	-149.90	4103.
70	NAI	-1.27	36.80	5.70	58.00	705.
	NAI	-1.27	36.80	-61.20	-27.80	2298.
	NAI	-1.72	36.80	47.80	16.10	1748.
	NAI	-1.27	36.80	39.80	48.80	1377.
	NAI	-1.27	36.80	30.60	-42.00	2522.
	NAI	-1.27	36.80	23.60	121.70	2694.
	NAI	-1.27	36.80	-4.40	153.10	3449.
	NAI	-1.27	36.80	-2.00	-12.80	1539.
	NDI	28.68	77.22	72.20	1.70	2093.
	NDI	28.68	77.22	-37.40	78.30	1958.
80	NDI	28.68	77.22	79.50	3.90	2108.

(to be continued)

Table 1. (continued)

	NDI	28.68	77.22	86.70	68.70	2016.
	NHA	12.21	109.21	28.10	93.80	759.
	NHA	12.21	109.21	-15.00	66.80	1471.
	NHA	12.21	109.21	36.90	140.90	1208.
	NHA	12.21	109.21	54.80	161.70	1926.
	PAS	34.15	-118.17	12.50	125.50	2908.
	PAS	34.15	-118.17	-4.50	135.00	3000.
	PAS	34.15	-118.17	-6.00	147.80	2740.
	PAS	34.15	-118.17	-17.50	167.50	2429.
90	PAS	34.15	-118.17	-22.00	169.50	2520.
	PAS	34.15	-118.17	-22.00	-174.00	2130.
	PAS	34.15	-118.17	-62.00	153.00	3280.
	PAS	34.15	-118.17	-55.00	-152.00	2575.
	PRE	-25.75	28.25	2.90	65.70	1365.
	PRE	-25.75	28.25	19.10	-63.70	2882.
	PRE	-25.75	28.25	26.70	-44.60	2528.
	PRE	-25.75	28.25	-45.60	96.10	1647.
	QUE	30.19	66.95	71.20	130.20	1901.
	QUE	30.19	66.95	46.70	-27.50	2331.
100	QUE	30.19	66.95	54.80	161.70	2379.
	QUE	30.19	66.95	39.50	141.80	2193.
	SBA	-77.85	166.77	-15.20	-173.50	1727.
	SEO	37.57	126.97	78.20	126.60	1336.
	SHI	29.51	52.53	-37.40	78.30	2177.
	SHI	29.51	52.53	78.20	126.60	2024.
	SHI	29.51	52.53	71.20	130.20	2023.
	SHI	29.51	52.53	39.50	141.80	2578.
	SHL	25.57	91.88	30.60	-42.00	3712.
	SHL	25.57	91.88	-15.00	66.80	1392.
110	SPA	-90.00	-0.0	51.20	-171.30	3922.
	STU	48.77	9.28	78.20	126.60	1612.
	SUV	-18.15	178.46	39.50	143.00	1850.
	SUV	-18.15	178.46	45.50	151.00	1900.
	SUV	-18.15	178.46	56.00	162.50	2030.
	SUV	-18.15	178.46	51.00	-173.00	1914.
	SUV	-18.15	178.46	40.00	-126.60	2161.
	SUV	-18.15	178.46	26.50	-111.00	2260.
	SUV	-18.15	178.46	17.50	-97.00	2520.
	SUV	-18.15	178.46	-38.00	-73.50	2590.
120	SUV	-18.15	178.46	-58.00	-67.00	2427.
	SUV	-18.15	178.46	-61.50	154.00	1350.
	SUV	-18.15	178.46	-7.40	130.70	1450.
	TAU	-42.91	147.32	-56.00	-121.50	1562.
	TKB	36.21	140.11	-57.00	147.00	2867.
	TKB	36.21	140.11	-15.00	-75.00	3960.
	TKB	36.21	140.11	-58.00	-67.00	4304.
	TKB	36.21	140.11	-15.00	-174.50	1870.
	TKB	36.21	140.11	-16.00	-172.00	1940.
	TKB	36.21	140.11	-42.00	173.00	2460.
130	TKB	36.21	140.11	-12.40	166.30	1550.
	TRI	45.71	13.76	72.20	1.70	883.
	TRI	45.71	13.76	37.50	73.40	1552.
	TRN	10.65	-61.40	-58.50	-25.10	2319.
	UME	63.81	20.24	-57.60	148.50	5209.
	UME	63.81	20.24	-55.90	-27.70	3866.
	UME	63.81	20.24	3.00	126.60	3279.
	UPP	59.86	17.63	52.40	174.50	2100.
	UPP	59.86	17.63	51.30	-179.70	2123.
	UPP	59.86	17.63	59.80	-150.60	1844.
140	UPP	59.86	17.63	52.20	-170.80	2136.
	UPP	59.86	17.63	52.30	177.70	2100.
	UPP	59.86	17.63	-44.20	38.10	3340.
	UPP	59.86	17.63	56.30	-153.90	1981.
	VAL	51.93	-10.25	-56.70	148.50	5049.
	VAL	51.93	-10.25	33.40	141.80	2955.
	VAL	51.93	-10.25	19.10	-63.70	1497.
	VAL	51.93	-10.25	72.10	1.40	655.
	VAL	51.93	-10.25	0.60	-25.90	1472.
	VAL	51.93	-10.25	-45.60	96.10	4191.
150	WIN	-22.57	17.10	-37.40	78.30	1603.
	WIN	-22.57	17.10	78.20	126.60	3803.
	WIN	-22.57	17.10	28.10	93.80	2781.
	WIN	-22.57	17.10	-0.10	124.50	3209.

method of least squares. By means of the expression (2) $v(\theta, \varphi)$ is calculated utilizing the parameters A_n^m and B_n^m just obtained.

Fig. 2. a

Fig. 2. a-b Surface elevation of the earth with the unit 100 m. Numerals in the figure are the elevation read from an atlas. (In order to avoid minus sign 100 is added.) The contours are drawn based on the values which are given by the synthesis $\sum_{N,M=0}^{4}(A_N^M \cdot P_N^M(\cos\theta)\cdot\cos M\varphi + B_N^M \cdot P_N^M(\cos\theta)\cdot\sin M\varphi)$. Synthesized values are not given in the figure. A_N^M and B_N^M, which are given in Table 3, are calculated based on the values in this figure and are used for the synthesis.

3. Data

Data in the present work is partly identical to that which was used in our previous work, while the remaining part was newly prepared using the micro-film seismogram of WWSSN. All the data are shown in Table 1. The travel time is that of the Rayleigh wave group velocity with the period 30 seconds (peak to peak, trough to trough), and the geodetic line connecting epicenters and stations are shown in Fig. 1.

Fig. 2. b

Table 2. Coefficients of expansion of $1/v(\theta, \varphi)$ into spherical surface harmonics A_N^M; $P_N^M(\cos\theta)\cdot\cos M\varphi$, B_N^M; $P_N^M(\cos\theta)\cdot\sin M\varphi$.

N	M	A_N^M	MEAN ERROR	B_N^M	MEAN ERROR
0	0	0.2688	0.0009		
1	0	0.0146	0.0027		
	1	0.0059	0.0013	0.0152	0.0016
2	0	0.0137	0.0039		
	1	0.0025	0.0013	0.0002	0.0016
	2	-0.1025	0.0006	-0.0013	0.0005
3	0	0.0039	0.0049		
	1	0.0028	0.0013	0.0030	0.0014
	2	-0.0013	0.0005	0.0016	0.0003
	3	0.0002	0.0002	0.0003	0.0002
4	0	-0.0038	0.0041		
	1	-0.0020	0.0014	-0.0013	0.0013
	2	-0.0008	0.0003	0.0020	0.0003
	3	0.0000	0.0000	-0.0003	0.0000
	4	0.0000	0.0000	0.0002	0.0000

Fig. 3. a

Table 3. Coefficients of the expansion of surface elevation of the earth into spherical surface harmonics A_N^M; $P_N^M(\cos\theta)\cdot\cos M\varphi$, B_N^M; $P_N^M(\cos\theta)\cdot\sin M\varphi$. Right half are the values based on A. E. H. Love's paper.

N	M	A_N^M	B_N^M	A_N^M	B_N^M
0	0	-2345			
1	0	1228		8.0	
	1	1038	523	16.5	9.5
2	0	1057		4.0	
	1	387	456	1.0	1.6667
	2	-265	-83	-2.3333	-1.3333
3	0	-402		-8.0	
	1	-159	86	-3.3333	-1.3333
	2	-135	177	0.0	1.7333
	3	19	89	-0.0667	0.9333
4	0	1228			
	1	-201	-234		
	2	-68	26		
	3	24	-5		
	4	0	10		

Fig. 3. b

Fig. 3 Synthesized group velocity distribution of Rayleigh waves with a period 30 seconds. Unit: 10 m/sec.

4. Numerical computation

Following the line given in § 2

$$C_n^m(\Theta, \Phi; \theta_k, \varphi_k) = \int_{(\theta, \varphi)}^{(\theta_k, \varphi_k)} P_n^m(\cos\theta) \cos m\varphi d\Delta$$
$$S_n^m(\Theta, \Phi; \theta_k, \varphi_k) = \int_{(\theta, \varphi)}^{(\theta_k, \varphi_k)} P_n^m(\cos\theta) \sin m\varphi d\Delta \qquad (5)$$
$$(k=1, 2, \cdots, N)$$

are calculated, which are the coefficients of observation equations. The right hand side of these equations are travel time t_k given in Table 1. Corresponding to one period we have a set of observation equations,

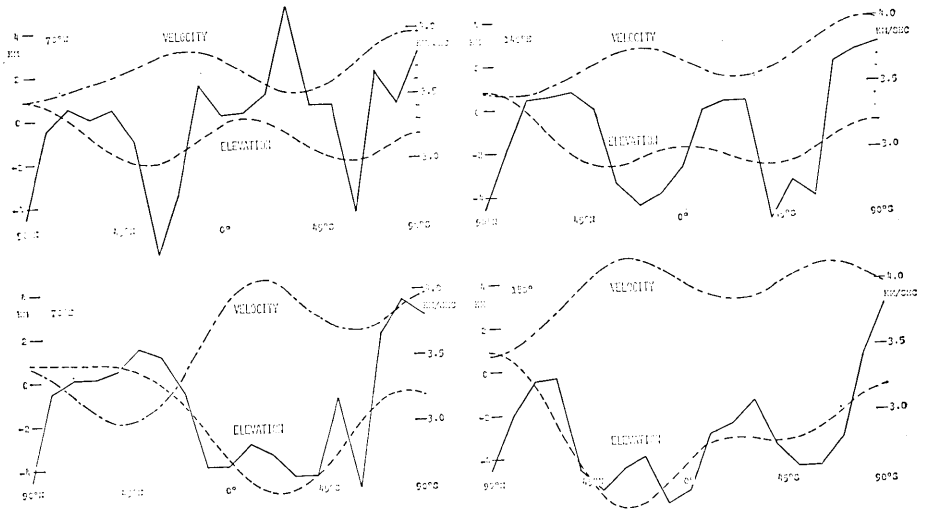

Fig. 4.

Surface elevation and group velocity along meridians. (Elevations of the north and south poles give no effect to the synthesized elevation.)

Solid line: Surface elevation read from an atlas.

Broken Line: Synthesized surface elevation based on the expression in the caption of Fig. 2.

Chain line: Group velocity as obtained in the present paper.

consequently a set of answers A_n^m and B_n^m is calculated. The values of A_n^m and B_n^m thus obtained are tabulated in Table 2. The errors are not necessarily very small, which fact might be inevitable from the nature of the problem.

In order to compare the velocity distribution with the topography the elevation of the earth's surface was expanded into spherical surface harmonics up to $n, m=4$. The coefficients obtained are given in Table 3. The data of surface elevation for this calculation is given in Fig. 2. A. E. H. Love[2] once tried a similar problem and calculated the coefficients for $n, m=0, 1, 2, 3$. These values also are given in Table 3 for reference.*

5. Results

The synthesized group velocity using the values of A_n^m and B_n^m in

2) A. E. H. LOVE, Gravitational Stability of the Earth," *Phil. Trans. A.* **207** (1907), 171. "Note on the Representation of the Earth's Surface by Means of Spherical Harmonics of the First Three Degree," *Proc. Roy. Soc. London A*, **80** (1908), 555. Some Problems of Geodynamics (1911).

A. Prey also treated a similar problem, *Abh. König. Ges. Wiss. Göttingen, Math.-Phys. Kl.*, N. F., **11** (1922), 3-20.

* Love did not use P_n^m functions, so the coefficients in his paper had to be modified so that they might be compared with the present work.

Table 2 is illustrated in Fig. 3 for the period 30 sec. This figure generally agrees with the world wide distribution recently compiled by one of the authors[3]. It is interesting to observe the correlation between the topography (Fig. 2, the contours being drawn based on the synthesis using the parameters in Table 3.) and the velocity distribution. This relation is also observed in Fig. 4 which gives cross sections along meridians. In the Pacific Ocean area the velocity maximum is remarkable. Further interesting points might be found in the figures if we observe carefully.

---

2. 世界中のレーリー波群速度の分布

地震研究所　佐　藤　泰　夫
国際地震・地震工学研修所　三　東　哲　夫

全世界にわたるレーリー波群速度の分布を表面球関数によって展開し，その係数を最小二乗法によって定めた．データはWWSSNのマイクロ・フィルム記録を使用した．求められた係数をつかってレーリー波の速度を合成し，その分布を同じく表面球関数を用いて表現した地形と比較すると，その相関の高いことが見られる．又さきに筆者の一人が求めた速度分布と大勢において一致する．

3) T. SANTÔ, *Zisin* [ii], **20** (1967), Special Issue, 43. (In Japanese)